



Kent Academic Repository

Le, N.C.H., Gubala, V., Gandhiraman, R.P., Coyle, C., Daniels, S. and Williams, D.E. (2010) *Total internal reflection ellipsometry as a label-free assessment method for optimization of the reactive surface of bioassay devices based on a functionalized cycloolefin polymer*. *Analytical and Bioanalytical Chemistry*, 398 (5). pp. 1927-1936. ISSN 1618-2642.

Downloaded from

<https://kar.kent.ac.uk/45234/> The University of Kent's Academic Repository KAR

The version of record is available from

<https://doi.org/10.1007/s00216-010-4099-4>

This document version

Pre-print

DOI for this version

Licence for this version

UNSPECIFIED

Additional information

Unmapped bibliographic data:LA - English [Field not mapped to EPrints]J2 - Anal. Bioanal. Chem. [Field not mapped to EPrints]C2 - 20803197 [Field not mapped to EPrints]AD - Biomedical Diagnostics Institute (BDI), Dublin City University, Dublin 9, Ireland [Field not mapped to EPrints]AD - National Centre for Plasma Science and Technology (NCPST), Dublin City University, Dublin 9, Ireland [Field not mapped to EPrints]AD - MacDiarmid Institute for Advanced Materials and Nanotechnology, Department of Chemistry, University of Auckland, Auckland 1142, New Zealand [Field not mapped to EPrints]DB - Scopus [Field not mapped to EPr...

Versions of research works

Versions of Record

If this version is the version of record, it is the same as the published version available on the publisher's web site. Cite as the published version.

Author Accepted Manuscripts

If this document is identified as the Author Accepted Manuscript it is the version after peer review but before type setting, copy editing or publisher branding. Cite as Surname, Initial. (Year) 'Title of article'. To be published in *Title of Journal*, Volume and issue numbers [peer-reviewed accepted version]. Available at: DOI or URL (Accessed: date).

Enquiries

If you have questions about this document contact ResearchSupport@kent.ac.uk. Please include the URL of the record in KAR. If you believe that your, or a third party's rights have been compromised through this document please see our [Take Down policy](https://www.kent.ac.uk/guides/kar-the-kent-academic-repository#policies) (available from <https://www.kent.ac.uk/guides/kar-the-kent-academic-repository#policies>).

Total internal reflection ellipsometry (TIRE) as a label-free detection technique for the monitoring of bioassays on a functionalized cyclo olefin polymer surface

Nam Cao Hoai Le^{1*}, Vladimir Gubala¹, Ram P. Gandhiraman¹, Conor Coyle^{1,2}, Stephen Daniels², David E. Williams^{1,3}

¹Biomedical Diagnostics Institute (BDI), Dublin City University, Dublin 9, Republic of Ireland

²National Centre for Plasma Science and Technology (NCPST), Dublin City University, Dublin 9, Republic of Ireland

³MacDiarmid Institute for Advanced Materials and Nanotechnology, Department of Chemistry, University of Auckland, Auckland-1142, New Zealand

*Corresponding author e-mail: nam.caohoaile@dcu.ie

Abstract: We report a label-free optical detection technique, called total internal reflection ellipsometry (TIRE), which can be applied to study the interactions between biomolecules and a functionalized polymer surface. Zeonor (ZR), a cyclo olefin polymer (COP) with low autofluorescence, high optical transmittance and excellent chemical resistance, is a highly suitable material for optical biosensor platforms due to the ease of fabrication. It can also be modified with a range of reactive chemical groups for surface functionalization. We demonstrate the applications of TIRE in monitoring DNA hybridization assays and human chorionic gonadotrophin (hCG) sandwich immunoassays on the ZR surface functionalized with carboxyl groups. The obtained Ψ and Δ spectra after the binding of each layer of analyte have been fitted to a four-layer ellipsometric model to quantitatively determine the amount of analytes bound specifically to the functionalized ZR surface. Our proposed TIRE technique with very low analyte consumption and its microfluidic array format could be a useful tool for evaluating several crucial parameters in immunoassays, DNA interactions, adsorption of biomolecules to solid surfaces or assessment of the reactivity of a functionalized polymer surface toward a specific analyte.

Keywords: Total internal reflection ellipsometry (TIRE), cyclo olefin polymer (COP), plasma enhanced chemical vapour deposition (PECVD), immunoassays, DNA hybridization, microfluidics.

1. Introduction

Zeonor (ZR), a type of cyclo olefin polymer (COP), with excellent optical and chemical properties and good machinability, has received increasing attraction by the biomedical diagnostics industry to develop low-cost, disposable biosensor platforms, appropriate for point of care applications [1-2]. Pristine ZR substrates are chemically inert and therefore need to be modified to have suitable physicochemical properties for biosensor applications. Surface functionalization of ZR to introduce chemical functional groups for immobilizing of proteins or oligonucleotides is a critical step toward the realization of low-cost biosensors.

Several techniques have been proposed to functionalize ZR with carboxylic or amine functional groups using both standard liquid phase chemistry as well as plasma enhanced chemical vapour deposition (PECVD) [3-9]. The quality of the functional films produced on ZR surface has a significant influence on the performance of the biosensor devices. In the above-mentioned reports, fluorescence detection has been used as the principal method to evaluate the reactivity of the functional films to target biomolecules. Quantitative data about the number of bound molecules from these experiments are usually deduced from fluorescence intensity data. However, the attachment of the fluorophores to a biomolecule is a time- and material-consuming process, which can frustrate the need to perform rapid and efficient assessments of the quality of the surface chemistry with respect to its use with specific reagents. Accordingly, for this purpose, a label-free detection method could be an advantageous alternative to fluorescence detection methods [10]. Surface plasmon resonance (SPR) has been widely applied as a label-free detection technique to study the interactions of molecules to functionalized gold surfaces [11-12] as well as to polymer surfaces [13-15]. Recently, total internal reflection ellipsometry (TIRE) or surface plasmon enhanced ellipsometry (SPEE) has been proposed as an alternative label-free method to detect the binding of

various analytes to a metal surface, typically gold [16-24]. Here, we propose to apply TIRE to monitor the binding of the biomolecules to a ZR surface functionalized with film containing carboxyl groups. A specialized PMMA microfluidic flow-cell has been developed allowing us to significantly reduce the volumes of analytes and amount of gold-based sensing substrates used in the experiments. The objective of this study has been to develop an efficient method for assessing both surface activation treatments and new bio-reagents applied to these surfaces, in a format where the surfaces reasonably resemble those that will be found in a final mass-produced device. The design has been specifically directed towards the assessment of single-chain antibodies prepared by phage display. To this end, we have successfully demonstrated the applications of TIRE in detection of two kinds of bioassays on the carboxyl functionalized ZR surface including DNA hybridization assay and human chorionic gonadotrophin (hCG) sandwich immunoassays. Together with fitting of the measured Ψ and Δ data, this method allows us to quantitatively estimate the surface excess of biomolecules bound to the functionalized ZR surface. This method also provides information about the stability of functionalized polymer surfaces upon contact with aqueous solutions as well as the reactivity of those surfaces toward a specific analyte, both of which are important to improve the performance of ZR-based biosensor devices.

2. Experimental

2.1 Materials

COP slides (Zeonor® 1060R) (ZR) (25 mm × 75 mm, 1 mm thick) were supplied by Åmic AB (Uppsala, Sweden). Gold-coated standard glass slides (Ti/Au = 2 nm/48 nm, 26 mm × 76 mm, 1 mm thick) were purchased from Phasis Sarl (Geneva, Switzerland). N-(3-dimethylaminopropyl)-N'-ethylcarbodiimide hydrochloride (EDC), N-Hydroxysuccinimide (NHS), and xylene were purchased from Sigma Aldrich (Dublin, Ireland). All chemicals were used as received without further purification. Amino modified single stranded DNAs (5'-ACG-GCA-GTG-TTT-AGC-3') (*Sal19* ssDNA, 15-mer), complementary single stranded DNAs (5'-GCT-AAA-CAC-TGC-CGT-3') (*Sal19 rev comp* ssDNA, 15-mer) and non-complementary single strand DNAs (5'-AAG-TTT-CTT-CTA-AAC-AGA CT-3') (*Sa20 non-comp* ssDNA, 20-mer) were purchased from Eurofins MWG Operon (Ebersberg, Germany). The antibodies and antigen used in this work were anti- α -human chorionic gonadotropin (hCG) (clone 3299:4), anti- β -hCG (clone 3468:2) and hCG (B250K/620; 250,000 mIU/ml) kindly donated by Inverness Medical Innovations (Bedford, UK).

2.2 Preparation of sensing substrate

A scheme for preparation of the sensing substrate is illustrated in Fig. 1. A COP slide was cut into small pieces and dissolved in xylene at 0.25 wt% w/v to make the raw ZR solution. The ZR solution was then filtered through a PTFE filter (pore size 0.2 μ m) (Chromafil Xtra PTFE-20/25 Macherey-Nagel, Duren, Germany) to eliminate the precipitates and dust particles. The ZR solution was then spin coated onto the Au-coated glass slide at 1300 rpm in 30 sec with acceleration in 2 sec and 2000 rpm in 5 sec with acceleration in 2 sec. The solvent xylene was naturally evaporated, leaving a thin ZR film [25]. The substrate was subsequently treated in an oxygen plasma for 1 min and then the carboxylic acid functionalised coatings were prepared by sequential deposition of Tetraethylorthosilicate (TEOS) and acrylic acid (AA) by low temperature Plasma Enhanced Chemical Vapor Deposition (PECVD). The resulting substrates exhibited increased COOH functionality for protein adhesion, an improved signal to noise ratios and a high resistance to washing. Given the nature of the technique, the details of the reaction mechanism is unclear. However, we hypothesize that the TEOS molecules are initially forming a thin bonding layer to cyclo olefin polymer, onto which acrylic acid is further polymerized. The polymerization process is initialized and assisted by plasma and results into a fabrication of relatively homogeneous layer with high density of carboxylic acids. The very low water contact angle of the film is also suggesting that TEOS might be inserted into the sensing -COOH layer, cross linking the polymerized AA molecules and forming abundance of silanols and silyl-ethers [26].

At different stages of the preparation of the sensing substrates, the wettability and the thickness of the deposited films were analyzed. The film wettability was analyzed by measuring the water contact angle using the First Ten

Angstroms FTA200 (Portsmouth, VA, USA) contact angle analyser. A high purity HPLC grade water (Sigma Aldrich, Dublin, Ireland) was used for the measurements. Images of drops were recorded with a CCD camera and analysed using the accompanied software. The thickness of the films deposited on the sensing substrate were measured by an UVISEL spectroscopic ellipsometer (Jobin Yvon Horiba, France) in external mode. A three-layer model (BK 7 glass, Au and add layer) was used in the fitting with PsiDelta 2 software (Jobin Yvon Horiba, France) to obtain the thickness of each layer from the measured Ψ and Δ spectra. The refractive indices of BK 7, Au and add layer are detailed in Section 3.4.

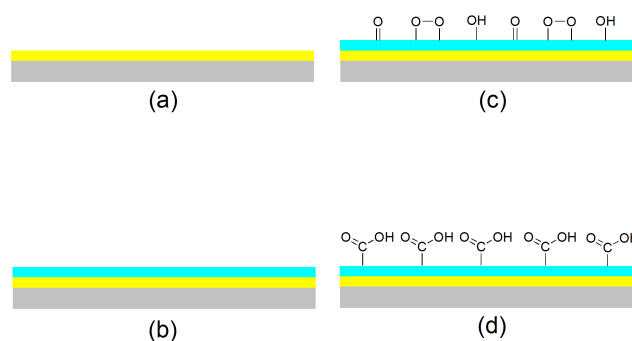


Fig. 1. Scheme for preparation of the sensing substrate containing carboxyl functional groups (a) Au-coated glass slide, (b) ZR spin-coating, (c) oxygen plasma treatment, (d) COOH film deposition (only the top layer of the film is illustrated).

2.3 Microfluidic flow-cell fabrication

The microfluidic flow-cell, containing four layers, was fabricated in poly(methyl methacrylate) (PMMA) and pressure-sensitive adhesive (PSA) using a CO₂ ablation laser machining system (Fig. 2). The top PSA layer, 50 μm in thickness, contains five reaction microwells glued with the sensing substrate on top and a PMMA (250 μm in thickness) connecting hole layer at the bottom. Inlets and outlets were also defined on this PMMA layer. Next is a PSA channel layer, also 50 μm in thickness, containing five sets of channels (500 μm in width) to connect the inlets and outlets to the reaction microwells through the PMMA connecting hole layer. Underneath is a base PMMA layer (250 μm in thickness) to seal the above PSA channel layer. Punched slabs of poly(dimethylsiloxane) (PDMS) (4 mm \times 4 mm \times 3 mm) as connectors were glued at the outlets of the top PMMA layer using PSA. With this design, we were able to incorporate five reaction microwells onto a sensing substrate which is a half of a gold-coated standard glass slide (26 mm \times 76 mm). Furthermore, the volume of the microwells were substantially reduced to approximately 4.7 μl compared to a typical few millilitres in previous works [16-22]. This feature is very important for experiments requiring expensive analytes like proteins or oligonucleotides.

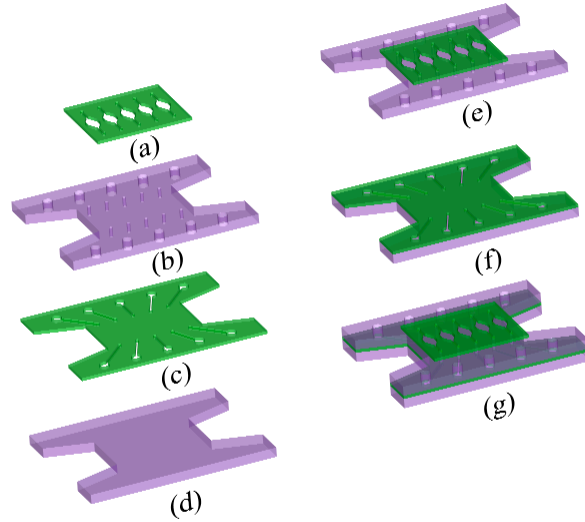


Fig. 2. Fabrication process of microfluidic flow-cell in PMMA and PSA (a) top PSA layer containing five reaction microwells, volume of each microwell is 4.7 μl , (b) connecting hole PMMA layer, (c) PSA channel layer, (d) bottom PMMA layer, (e) bonding of top PSA layer and connecting hole PMMA layer, (f) bonding of PSA channel layer and bottom PMMA layer, (g) complete four-layer microfluidic flow-cell.

2.4 TIRE experimental setup

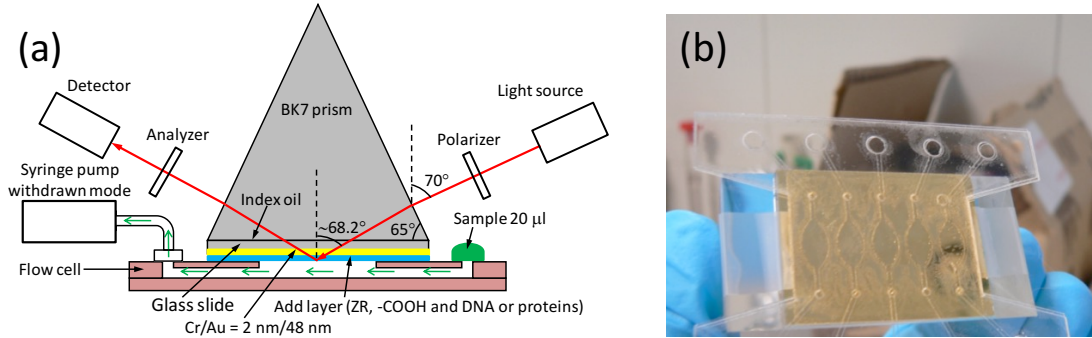


Fig. 3. (a) TIRE experimental setup fitted on an UVISEL spectroscopic ellipsometer and a Harvard Apparatus syringe pump (b) Assembly of the prism, the sensing substrate and the five-microwell flow-cell.

Total internal reflection ellipsometry (TIRE) or surface plasmon enhanced ellipsometry (SPEE) is a spectroscopic ellipsometry measurement method operated under the total internal reflection (TIR) condition [16-24]. As in a conventional spectroscopic ellipsometry method, TIRE also measure two ellipsometric angles Ψ and Δ versus wavelengths. These Ψ and Δ values are defined by the ratio ρ of the reflection coefficients R_p and R_s for components of light polarized parallel $-p$ and perpendicular $-s$ to the plane of incidence following the ellipsometry equation [27].

$$\rho = \frac{R_p}{R_s} = \tan \Psi \exp(i\Delta) \quad (1)$$

It is obvious that Ψ and Δ also depend on angle of incidence Φ and wavelengths λ . The refractive indices and thicknesses of each layer of the reflecting surfaces can be found by fitting the measured Ψ and Δ data to a defined model.

Our TIRE experimental setup was based on an UVISEL spectroscopic ellipsometer (Jobin Yvon Horiba, France) (Fig. 3(a)). The sensing substrate was first glued to the fabricated microfluidic flow-cell by adhesion of the PSA

reaction microwell layer. A BK7 prism was placed on top of the sensing substrate with an intermediate refractive index matching oil and secured by tapes (Fig. 3(b)). A syringe pump (Harvard Apparatus, Boston, USA) is connected to the outlet of one microwell of the flow-cell through a polymer tubing and a PDMS connector. A droplet of analyte (20-30 μl) injected at the corresponding inlet, was sucked into the microwell by the syringe pump operating under the withdrawn mode [28]. The flow rate was controlled within 4 to 5 $\mu\text{l}/\text{min}$. The volume of analyte is always larger than the volume of the microwell (4.7 μl) to make sure the microwell is always filled with analyte and is not dried during measurements. TIRE measurements were conducted at an external angle of incidence of 70° with wavelengths ranging from 400 nm to 850 nm. After refracting at the air/BK7 prism interface, the light rays enter the interface of the sensing substrate and the aqueous buffer at an angle of incidence ranging from 68.263° to 68.308° (for wavelengths from 400 nm to 850 nm) due to the dispersion at the air/BK7 interface. If the wavelength range is broader, the variation in the incident angles is larger and could cause some distortion in the detected signals since the detector will receive the reflected light beams at different reflecting angles. However, with this current wavelength range, the variation in incident angles is negligible and in fact we have not detected any distortion in our measured Ψ and Δ signals. The integration time was 200 ms and the spectral resolution varied from 2 nm to 10 nm. Although the flow-cell contains five microwells, only one assay was performed at a time on one microwell to prevent any possible shifting of the light rays in the optical setup. In all experiments, the Ψ and Δ spectra were always recorded after the syringe pump was turned off and the measuring microwell was filled with phosphate buffer saline (PBS, pH 7.4). PsiDelta 2 software (Jobin Yvon Horiba, France) was used for fitting the data from the measured Ψ and Δ spectra from TIRE.

2.5 TIRE experimental procedure

First, we tested the stability of the COOH film on the sensing substrate inside one of the microwells by replacing new PBS buffer every 60 min in a 120 min period during which three sets of Ψ and Δ were recorded separated by 60 min. Three sets of Ψ and Δ spectra were superimposed on the same plot to check if they still remained overlapped.

The DNA hybridization assay was conducted in a fresh microwell after the baseline Ψ and Δ spectra of the COOH surface in PBS buffer were recorded. 30 μl of aminated *Sa19* ssDNA at a concentration of 10^{-5} M in 100 mM EDC in 2-(*N*-morpholino)ethanesulfonic acid (MES, pH 8.0) buffer was then pumped into the microwell and allowed to react for 60 min (Fig. 4(b-c)). A second set of Ψ and Δ spectra, which correspond to the registration of the binding of the capture *Sa19* ssDNA, were measured after the microwell was rinsed with 50 μl of PBS buffer. Next, 30 μl of complementary *Sa19 rev comp* ssDNA at concentration of 10^{-5} M in hybridization buffer (150 mM NaCl, 150 mM saline-sodium citrate (SSC) buffer) pH 7.0) was pumped into the microwell and also allowed to react for 60 min before rinsing with 50 μl PBS. A third set of Ψ and Δ spectra were then recorded corresponding to the registration of the complementary *Sa19 rev comp* ssDNA to the capture *Sa19* ssDNA. We also conducted two negative control experiments in two different microwells. The first negative control experiment was conducted with mismatched *Sa20 non-comp* ssDNA at concentration of 10^{-5} M in the same hybridization buffer to confirm the specificity of the captured ssDNA probes. The second negative experiment was performed to assess the capture efficiency of the aminated *Sa19* ssDNA to the COOH surface without EDC in the MES buffer.

For hCG sandwich immunoassays, the baseline Ψ and Δ spectra of the COOH surface in PBS were also recorded first. The reaction microwell was then activated by 100 mM EDC and 100 mM NHS in DI water for 15 min and then rinsed by 50 μl of PBS. 30 μl of capture anti- α -hCG antibody in PBS (pH 7.4) at a concentration of either 2 or 20 or 200 $\mu\text{g}/\text{ml}$ was pumped into the microwell and allowed to react for 30 min before rinsing with 50 μl PBS (Fig. 4(b-d)). Ψ and Δ spectra of bound anti- α -hCG on COOH surface were then measured. 30 μl of hCG solution in PBS at fixed concentration of 2 $\mu\text{g}/\text{ml}$ was then injected and also allowed to react with the surface-bound anti- α -hCG for 30 min. A third set of Ψ and Δ spectra were recorded after the microwell was rinsed with 50 μl PBS. Finally, 30 μl solution of anti- β -hCG in PBS at the same concentration as that of the

capture anti- α -hCG was pumped in, allowed to react for 30 min and rinsed with 50 μ l PBS before the fourth set of Ψ and Δ spectra were measured.

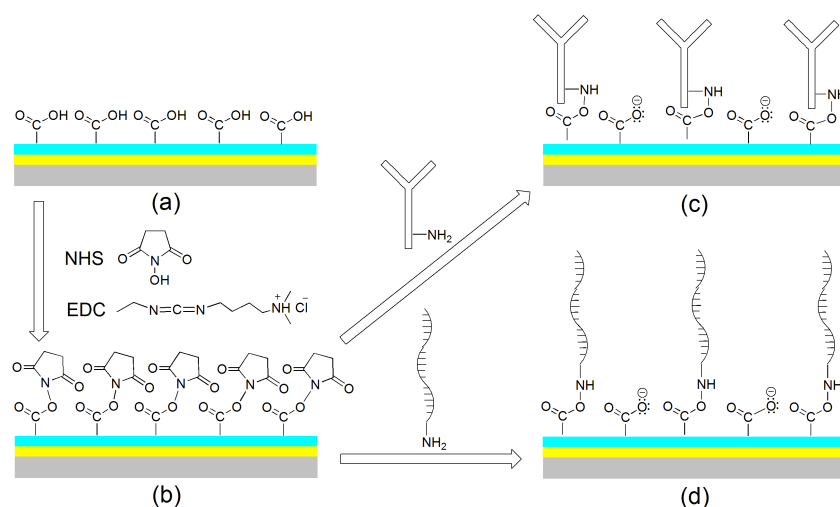


Fig. 4 (a-b) A scheme for activation of COOH surface (only the top layer of the film is illustrated) by EDC (for ssDNA) or EDC/NHS (for antibody), (c) binding to the activated COOH surface by antibody anti- α -hCG, (d) or by aminated *Sa19* ssDNA.

3. Results and discussion

3.1. Water contact angle, film thicknesses and stability of sensing substrate

The water contact angle changes after the deposition of ZR and after the introduction of COOH groups on the Au-coated glass slide are plotted on Fig. 5(a). The deposition of ZR caused a small increase in water contact angle due to the hydrophobic nature of ZR. However, after the deposition of COOH film, the water contact angle dropped substantially to approximately 23°. This change in contact angle is attributed to the hydrophilic characteristic of the COOH functional groups. Spectroscopic ellipsometric measurements were performed to confirm the successful deposition of ZR and COOH on Au-coated glass substrates (Fig 5(b)). After ZR deposition, the original Δ spectrum shifted downward from “Au” to “ZR/Au”. The ellipsometric fitting confirmed that a ZR layer of 9.8 nm was successfully deposited on the Au slide. However, the thickness of the ZR layer was reduced to 4.9 nm (not shown) after being treated in oxygen plasma for 1 min at 60 W before the deposition of COOH film [25]. Next, the downward shift of Δ spectrum from “ZR/Au” to “COOH/ZR/Au” corresponded to an increase in thickness of 4.7 nm, which was caused by the deposition of the functional COOH film onto the ZR-coated Au-coated glass surface. These water contact angle and spectroscopic ellipsometry measurements confirmed the presence of ZR and COOH films on the sensing substrate. The superimposition of three sets of Ψ and Δ spectra of COOH film on the sensing substrate measured under TIRE mode over 120 min showed that no shift of any spectra were detected (Fig. 6). Since there was no change in refractive index within the solid/liquid interface, the overlap of the spectra confirmed the stability in the thickness of the COOH film upon contact with aqueous PBS buffer.

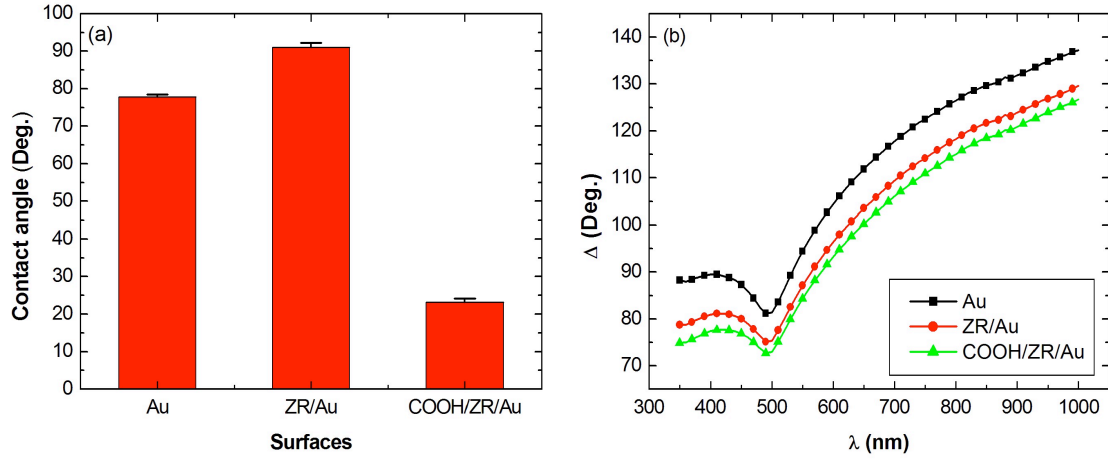


Fig. 5. (a) Surface contact angle changes on Au-coated glass slide after spincoating ZR and then introduction of COOH functional film (b) corresponding Δ spectra shift after ZR spin-coating (before plasma treatment) and COOH film deposition.

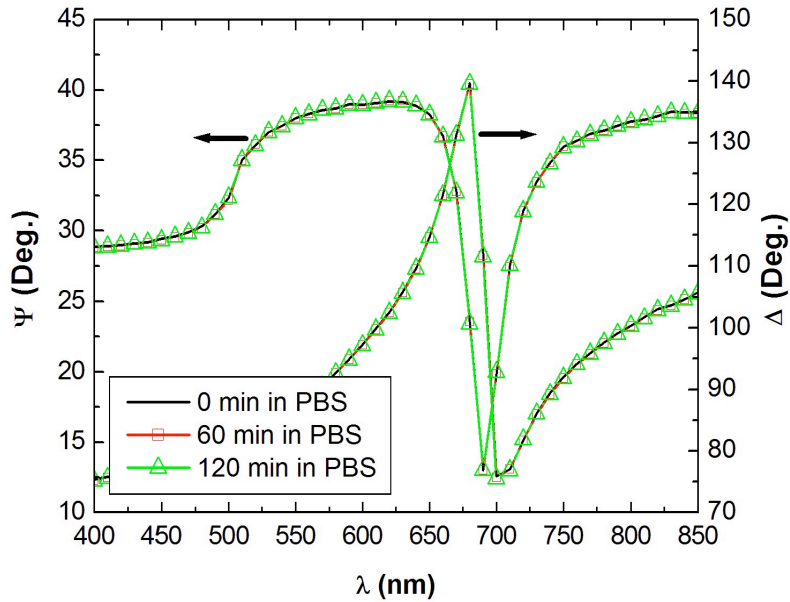
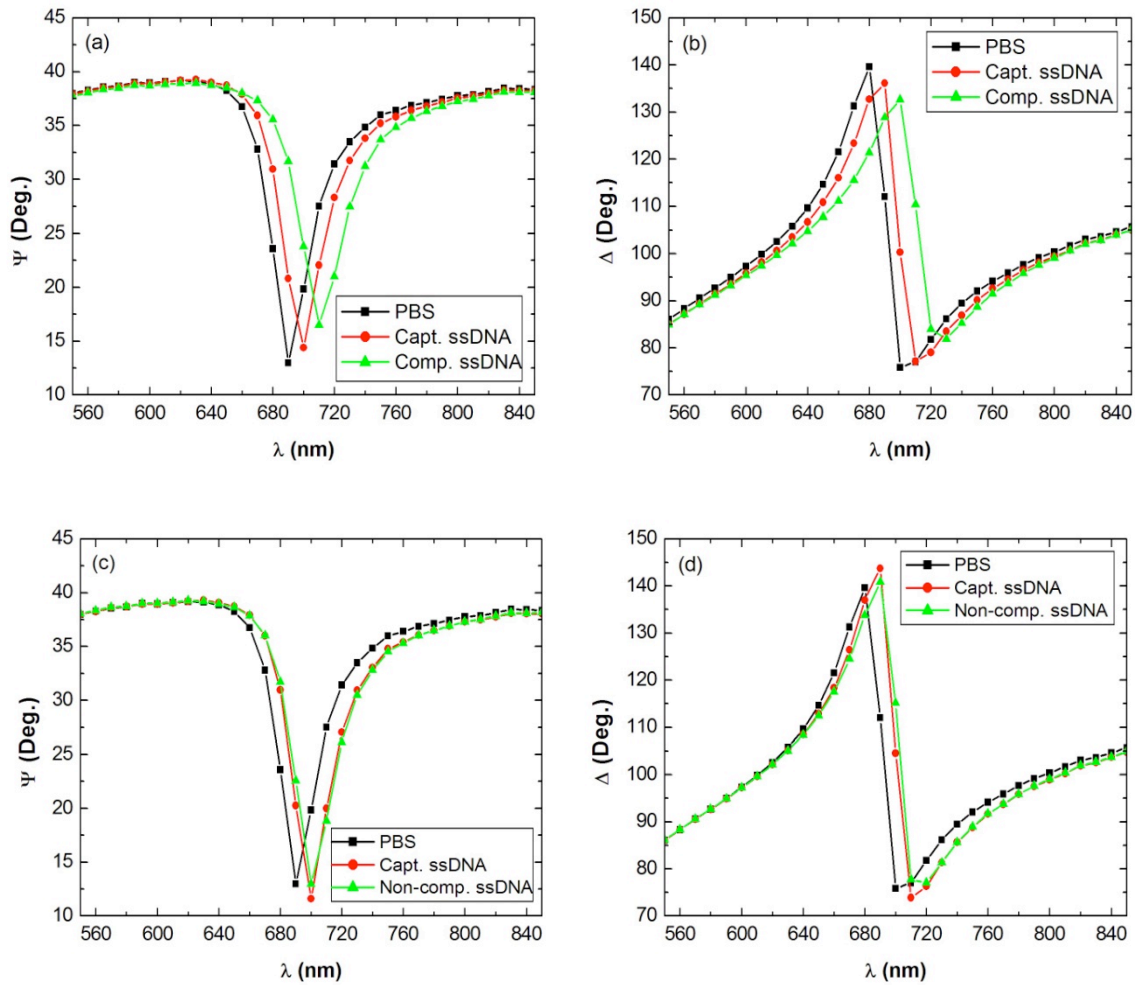


Fig. 6. Superimposition of three set of Ψ and Δ spectra of COOH film on the sensing substrate in contact with PBS buffer (pH 7.4) measured over a period of 120 min separated by 60 min.

3.2. DNA hybridization assays

Ψ and Δ spectra of the complete DNA hybridization assay are plotted in Fig. 7(a-b), respectively. The introduction of the capture aminated *Sa19* ssDNA (15-mer) solution and then the complementary *Sa19 rev comp* ssDNA (15-mer) solution resulted in large shifts in both Ψ and Δ spectra from the initial Ψ and Δ spectra of the COOH surface when the microwell was filled with PBS buffer. In the first negative control experiment, a mismatched *Sa20 non-comp* ssDNA solution (20-mer) was incubated for 60 min after the capture *Sa19* ssDNA had been immobilized to assess the non-specific hybridization and non-specific binding effect. As seen in Fig. 7(c-d), the introduction of the non-complementary ssDNA solution did not result in any shifts in the Ψ and Δ spectra. Therefore, the effects of non-specific binding and hybridization were minimal. The second negative control experiment, conducted by incubating the aminated *Sa19* ssDNA solution without activating agent EDC, showed that only a very small shift in Ψ and Δ spectra were observed after 60 min (Fig. 7(e-f)). A four-layer

ellipsometric model as presented in Table 1, Section 3.4 has been used for fitting of the measured Ψ and Δ spectra to deduce the effective thickness of each DNA layer. It has been found that only a small amount of aminated *SalI* ssDNA, 0.25 ± 0.12 (nm) in thickness, was captured on the COOH surface for the second negative experiment. For the positive experiment, fitting of Ψ and Δ spectra also gave effective thicknesses of both the capture ssDNA and the hybridized DNA of 2.02 ± 0.16 (nm) and 3.49 ± 0.42 (nm), respectively. It is interesting to note that the hybridization resulted in an increase in effective thickness. This suggests that the capture ssDNA could form a layer composed of coiled oligonucleotides, which are being stretched out during the hybridization to its complementary strand. This observation is in good agreement with results previously reported in the literature [29-30].



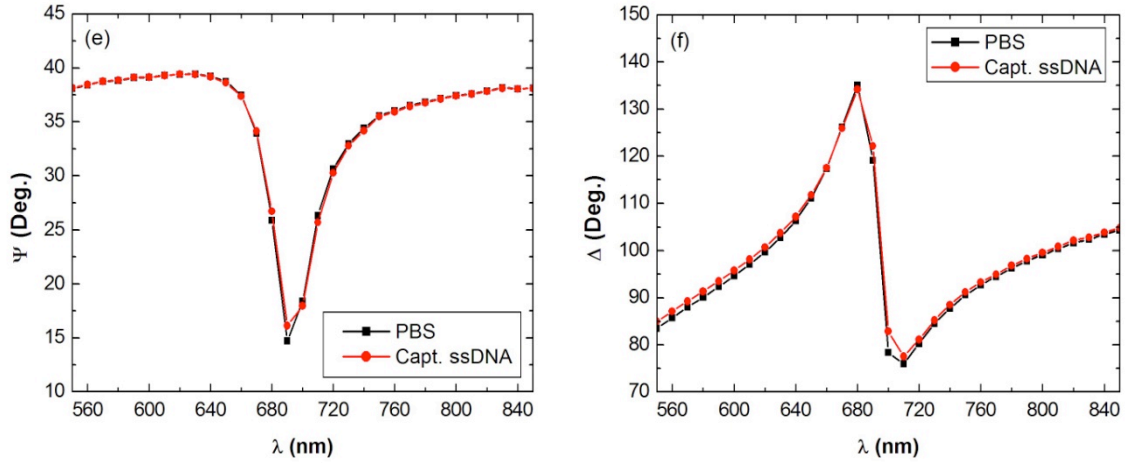


Fig. 7. (a-b) Ψ and Δ spectral shifts after binding of the capture of aminated *Sal9* ssDNA (15-mer) at 10^{-5} M and hybridized with complementary *Sal9 rev comp* ssDNA (15-mer) at 10^{-5} M. (c-d) Ψ and Δ spectral shifts were only observed for binding of the capture *Sal9* ssDNA (15-mer) at 10^{-5} M but not for the mismatched *Sa20 non-comp* ssDNA (20-mer) at 10^{-5} M (e-f) Capture of aminated *Sal9* ssDNA (15-mer) at 10^{-5} M without EDC activation, Ψ and Δ spectral shift were minimal.

3.3. hCG sandwich immunoassays

Similarly to the DNA hybridization assays, the hCG sandwich immunoassays were successfully realised after activating the COOH surface with EDC/NHS mixture inside the TIRE microwells. The covalent binding of the capture anti- α -hCG antibody caused a large and distinct shift in both Ψ and Δ spectra. These shifts increased with increasing concentration of the anti- α -hCG, in the range from 2 to 200 $\mu\text{g/ml}$ (Fig. 8(a-f)). It is noticeable to see that the original plasmon resonance wavelength for these assays (i.e. 727.5 nm) was different than that in the DNA hybridization assay above (i.e. 690 nm). This difference could be due to the difference in COOH film thickness deposited each time when the sensing substrate is prepared. The COOH thickness in the case of DNA hybridization assay was approximately 4.7 nm while that for the hCG assay was approximately 6.7 nm. The subsequent binding of the hCG antigen at 2 $\mu\text{g/ml}$ to the capture anti- α -hCG caused another shift in both Ψ and Δ spectra (Fig. 8(a-f)). Finally, the binding of the second antibody anti- β -hCG caused a third shift in both Ψ and Δ spectra (Fig. 8(a-f)). Compared to the first shift after binding of anti- α -hCG, the second and the final shifts in the Ψ and Δ spectra for binding of hCG and anti- β -hCG, respectively, were small and not so distinctive. We reason that, similarly to the case of adsorption of anti- β -hCG to a silica surface, here the first anti- α -hCG antibodies could predominantly bind to COOH film with the same lying down or “flat-on” orientation fashion and they were arranged like a disordered stack of dish plates [35]. The antigen hCG then filled in some of the gaps and contributed some more dish plates lying in and on the first layer of anti- α -hCG antibodies. Similarly, the second anti- β -hCG antibody filled in more of the remaining gaps. Hence the apparent thickness change was small, corresponding to the small shifts in the Ψ and Δ spectra after the binding of hCG and anti- β -hCG. Similar reasoning concerning the changes in molecular conformation on the surface could also explain why, for the case of the DNA hybridization assay, the shift in Ψ and Δ spectra after binding of the complementary ssDNA were still relatively large compared to those of the capture ssDNA (Fig. 7(a-b)). This large shifts could be due to the possibility that the DNA strands were stretched out upon hybridization unlike the “fill-in” fashion upon binding of antigen and antibody. However, there should further investigations using complementary techniques like atomic force microscopy (AFM) or neutron reflectivity to study the actual orientation of the proteins using forming complex sandwich immunoassays the ZR surface [35]. Several optical detection methods have been proposed to detect hCG in sandwich immunoassays with very high sensitivity [31-34]. The concentration of hCG in the current work was still relatively high: however it has been shown that TIRE can successfully be applied to detect hCG capture and labelling in sandwich immunoassays. For further improvements in the

sensitivity, the optimal thickness of the gold film, the COOH film uniformity and non-specific binding of the analyte to the PMMA flow-cell surface need to be addressed.

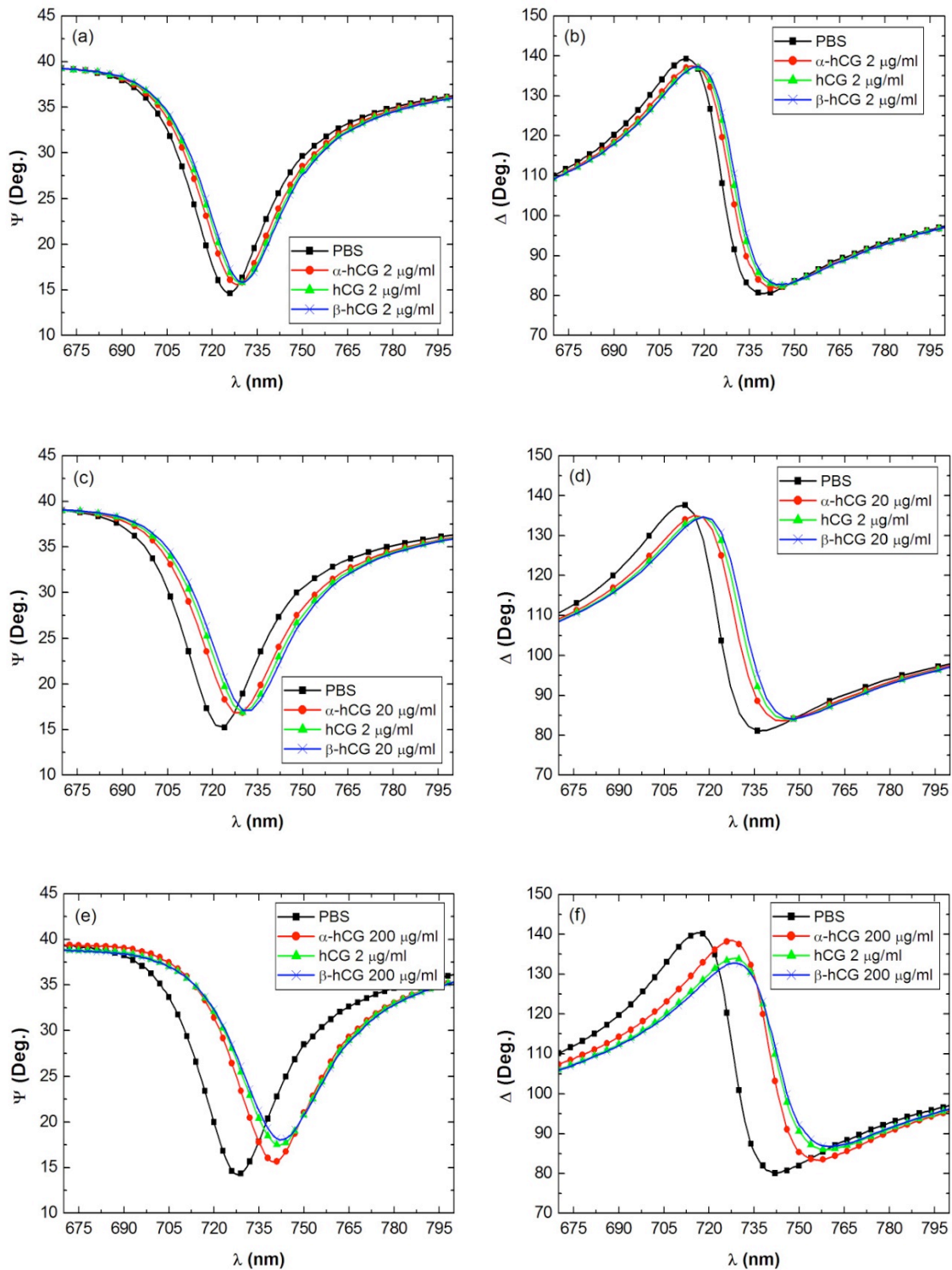


Fig. 8. Ψ and Δ spectral shifts for three hCG sandwich immunoassays after EDC/NHS activation, (a-b) anti- α -hCG and anti- β -hCG concentrations were 2 $\mu\text{g/ml}$, (c-d) anti- α -hCG and anti- β -hCG concentrations were 20 $\mu\text{g/ml}$, and (e-f) anti- α -hCG and anti- β -hCG concentrations were 200 $\mu\text{g/ml}$. hCG concentration for the three assays was fixed at 2 $\mu\text{g/ml}$.

3.4. Fitting data and calculate surface excess

A four-layer ellipsometric model summarized in Table 1 was used in the fitting of the measured Ψ and Δ spectra by using the PsiDelta 2 software (Jobin Yvon Horiba, France) to deduce the thickness of each add layer to the Au surface [19-22]. The refractive indices of all four layers in the model were fixed in the fitting model. The refractive index of the BK prism was obtained from SCHOTT BK7 datasheet. The refractive indices of Au and water were obtained from the software library based on Palik [36-37]. The refractive indices of the ZR film, the COOH film, and the DNA or the protein film are assumed to follow the same Cauchy dispersion formula obtained from [20]. This assumption inevitably undermined the exact refractive index of each add material layer but it helped to separate the coupling between refractive indices and film thicknesses in ellipsometric fitting [19-22, 38]. Accordingly, the thickness of the subsequent add layer, representing the plasma treated ZR film, the COOH film and the DNA or protein film, is increased when each film is built on to the Au surface. The thickness of Au was obtained from previous external spectroscopic ellipsometry and was fixed in the fitting. The only variable is the thickness of the organic or bio-layer layer including the ZR film, the COOH film and the DNA or the protein layer.

The thicknesses of the ZR film and the COOH have been found previously by measurement and fitting in the external mode (section 3.1). The thickness of the plasma treated ZR film (before COOH film deposition by PECVD) was found to be 4.9 nm. The thickness of the COOH film was 4.7 nm or 6.7 nm for sample used in DNA hybridization assay and hCG immunoassays, respectively. The total thickness of the ZR film and the COOH film was used as a lower limit to guide the software to find the thickness change during the fitting.

Table 1: Four-layer model used in the fitting of the measured Ψ and Δ spectra

Layer	Materials	Thickness	Refractive index (all fixed)
1	BK7	∞	SCHOTT BK7 data sheet
2	Au	52 nm (fixed)	Taken from Palik [36]
3	Add layer (ZR, COOH, DNA or protein)	variable	Cauchy: $A + B/\lambda^2 + C/\lambda^4$ [20] $A = 1.415, B = 0.01, C = 0$
4	Water	∞	Taken from Palik [37]

For DNA hybridization assays, we could only deduce the effective thickness changes after the immobilization of the capture ssDNA and then the hybridization of the complementary ssDNA as mentioned in Section 3.2. However, for the hCG immunoassays, the availability of the change of in the refractive index of the protein solution with increasing concentration enabled us to employ the De Feitjer's formula to determine the amount of bound proteins from their thicknesses [39].

$$\Gamma = \frac{\tau(n - n_w)}{dn/dc} \quad (2)$$

where Γ (mg/m^2) is the protein surface excess, τ is the thickness of the protein in \AA , n_w is the refractive index of the aqueous phase, n is the refractive index of the protein and dn/dc is the change in the refractive index of the protein solution with increasing concentration, which is close to $0.18 \text{ cm}^3/\text{g}$ for a variety of proteins [39]. The results of the fitting for three hCG immunoassays were summarized in Table 2.

Table 2: Fitting results and surface density calculation from three assays in Fig. 8

Assay	Surface excess of anti- α -hCG (mg/m ²)	Surface excess of hCG (mg/m ²)	Surface excess of anti- β -hCG (mg/m ²)
Fig. 8(a-b)	0.91 \pm 0.04	0.39 \pm 0.02	0.23 \pm 0.01
Fig. 8(c-d)	1.87 \pm 0.03	0.60 \pm 0.02	0.41 \pm 0.07
Fig. 8(e-f)	4.37 \pm 0.12	0.84 \pm 0.09	0.28 \pm 0.06

As expected, the surface excesses of the anti- α -hCG antibodies increased with increasing concentrations of the capture anti- α -hCG in the initial surface functionalisation. Similarly, surface excesses of the antigen hCG also increased with increasing surface excess of anti- α -hCG. However, this trend was somewhat discontinued for the detection antibody, anti- β -hCG. The surface excesses of anti- β -hCG do not follow any particular trend. There should be further investigations to understand the effects of the surface excesses of the first capture antibody and antigen on the surface excesses of the second antibody [38].

4. Conclusions

A label-free, low volume and in-situ TIRE detection technique to monitor the binding of biomolecules to a functionalized ZR surface in a microfluidic array format has been proposed. The design of a specialized PMMA flow-cell enabled us to fit five reaction microwells onto the sensing substrate, a half of a gold-coated standard glass slide. The volume of each microwell was only 4.7 μ l and the volume of analyte used for each reaction was 20 to 30 μ l, which is a useful parameter when screening through a large number of variable parameters of bioassays. Binding of each layer of biomolecules caused a spectral shift for both Ψ and Δ spectra. Ellipsometric modelling and fitting allowed us to quantify the surface excesses of the bound biomolecules. The proposed TIRE technique could be a very valuable tool for evaluating important parameters in immunoassays, DNA interactions, adsorption of biomolecules to solid surfaces or assessment of the reactivity of a functionalized polymer surface toward a specific analyte.

Acknowledgements

This material is based upon work supported by the Science Foundation Ireland under Grant No. 08/CE3/B754. D. E. Williams is an E.T.S. Walton Visiting Fellow of Science Foundation Ireland. Authors would like to thank Dr. J. Garcia-Cordero for helping with the design and fabrication of flow-cell. Authors also thank Dr. M. Stchakovsky and Dr. D. Sheppard from HORIBA Jobin Yvon for helping with the ellipsometric fitting.

References

- [1] Kameoko J., Craighead H.G., Zhang, H., Henion J. A., Polymeric microfluidic chip for CE/MS determination of small molecules, *Anal. Chem.*, 2001,73, 1935-1941
- [2] Diaz-Quijada G. A., Peytavi R., Nantel A., Roy E., Bergeron M. G., Dumoulin M. M., Veres T., Surface modification of thermoplastics—towards the plastic biochip for high throughput screening devices, *Lab Chip*, 2007, 7, 856-862.
- [3] Laib S., MacCraith B. D., Immobilization of biomolecules on cycloolefin polymer supports, *Anal. Chem.* 2007, 79, 6264-6270
- [4] Pu Q., Oyesanya O., Thompson B., Liu S, Alvarez J. C., On-chip micropatterning of plastic (cyclic olefin copolymer, COC) microfluidic channels for the fabrication of biomolecule microarrays using photografting methods, *Langmuir*, 2007, 23, 1577-1583
- [5] Jonsson C., Aronsson M., Rundstrom G., Pettersson C., Mendel-Hartvig I., Bakker J., Martinsson E., Liedberg B., MacCraith B., Ohman O., Melin J., Silane-dextran chemistry on lateral flow polymer chips for immunoassays, *Lab Chip*, 2008, 8, 1191–1197

- [6] Raj J., Herzog G., Manning M., Volcke C., MacCraith B. D., Ballantyne S., Thompson M., Arrigan D. W. M., Surface immobilisation of antibody on cyclic olefin copolymer for sandwich Immunoassay, *Biosens. Bioelectron.*, 2009, 24, 2654–2658
- [7] Volcke C., Gandhiraman R. P., Gubala V., Raj J., Cummins T., Fonder G., Nooney R. I., Mekhalif Z., Herzog G., Daniels S., Arrigan D. W. M., Cafolla A. A., Williams D. E., Reactive amine surfaces for biosensor applications, prepared by plasma-enhanced chemical vapour modification of polyolefin materials, *Biosens. Bioelectron.* 2010, 25, 1875–1880
- [8] Gandhiraman R. P., Volcke C., Gubala V., Doyle C., Basabe-Desmots L., Dotzler C., Toney M. F., Iacono M., Nooney R. I., Daniels S., James B., Williams D. E., High efficiency amine functionalization of cycloolefin polymer surfaces for biodiagnostics, *J. Mater. Chem.*, 2010, 20, 4116-4127
- [9] Gubala V., Gandhiraman R. P., Volcke C., Doyle C., Coyle C., James B., Daniels S., Williams D. E., Functionalization of cycloolefin polymer surfaces by plasma-enhanced chemical vapour deposition: comprehensive characterization and analysis of the contact surface and the bulk of aminosiloxane coatings, *Analyst*, 2010, 135, 1375-1381
- [10] Haake H.-M., Schutz A., Gauglitz G., Label-free detection of biomolecular interaction by optical sensors, *Fresenius J. Anal. Chem.*, 2000, 366, 576–585.
- [11] Liedberg B., Nylander C., Lundström I., Biosensing with surface plasmon resonance—how it all started, *Biosens. Bioelectron.*, 1995, 10, I–IX.
- [12] Johansen K., Arwin H., Lundström I., Liedberg B., Imaging surface plasmon resonance sensor based on multiple wavelengths: sensitivity considerations, *Rev. Sci. Instrum.*, 2000, 71, 3530–3538.
- [13] Green R. J., Davies J., Davies M. C., Roberts C. J., Tendler S. J. B., Surface plasmon resonance for real time in situ analysis of protein adsorption to polymer surfaces, *Biomaterials*, 1997, 18, 405-413
- [14] Kugimiya A., Takeuchi T., Surface plasmon resonance sensor using molecularly imprinted polymer for detection of sialic acid, *Biosens. Bioelectron.*, 2001, 16, 1059-1062
- [15] Hook A. L. , Thissen H., Voelcker N. H., Surface plasmon resonance imaging of polymer microarrays to study protein–polymer interactions in high throughput, *Langmuir*, 2009, 25, 9173–9181
- [16] Westphal P, Bornmann A, Biomolecular detection by surface plasmon enhanced ellipsometry, *Sens. Actuators B*, 2002, 84, 278– 282.
- [17] Poksinski M., Arwin H., In situ monitoring of metal surfaces exposed to milk using total internal reflection ellipsometry, *Sens. Actuators B*, 2003, 94, 247-252
- [18] Arwin H., Poksinski M., Johansen K., Total internal reflection ellipsometry: principles and applications, *Appl. Opt.* 2004, 43, 3028–3036.
- [19] Poksinski M., Arwin H., Protein monolayers monitored by internal reflection ellipsometry, *Thin Solid Films*, 2004, 455–456C, 716–721
- [20] Nabok A., Tsargorodskaya A., Hassan A.K., Starodub N.F., Total internal reflection ellipsometry and SPR detection of low molecular weight environmental toxins, *Appl. Surf. Sci.* 2005, 246, 381–386.
- [21] Nabok A., Tsargorodskaya A., Davis F., Higson S.P.J., The study of genomic DNA adsorption and subsequent interactions using total internal reflection ellipsometry, *Biosens. Bioelectron.*, 2007, 23, 377–383.
- [22] Nabok A, Tsargorodskaya A., Holloway A, Starodub N. F., and Demchenko A., Specific binding of large aggregates of amphiphilic molecules to the respective antibodies, *Langmuir*, 2007, 23, 8485-8490

- [23] Basova T., Plyashkevich V., Hassan A., Gürek A. G., Gümüş G, Ahsen V, Phthalocyanine films as active layers of optical sensors for pentachlorophenol Detection, *Sens. Actuators B*, 2009, 139, 557–562
- [24] Balevicius Z., Vaicikauskas V., Babonas G.-J., The role of surface roughness in total internal reflection ellipsometry of hybrid systems, *Appl. Surf. Sci.* 256 (2009) 640–644
- [25] Larsson A., Ekblad T., Andersson O., Liedberg B., Photografted poly(ethylene glycol) matrix for affinity interaction studies, *Biomacromol.*, 2007, 8, 287-295
- [26] Coyle C., Gandiraman R. P., Gubala V., Le N. C. H., Swift P., Daniels S., Williams D. E., Tetraethyl orthosilicate and acrylic acid together forming robust carboxylic functionalities on cyclic olefin copolymers with reduced non specific binding, 2010, *to be submitted*
- [27] Azzam R.M.A., Bashara N.M., *Ellipsometry and polarized light*, North Holland, third printing, 1992.
- [28] Le N. C. H., Yokokawa R., Dao D. V., Nguyen T. D., Wells J. C., Sugiyama S., Versatile microfluidic total internal reflection (TIR)-based devices: Application to microbeads velocity measurement and single molecule detection with upright and inverted microscope, *Lab Chip*, 2009, 9, 244-250
- [29] Liebermann T., Knoll W., Sluka P., Herrmann R., Complement hybridization from solution to surface-attached probe-oligonucleotides observed by surface-plasmon-field-enhanced fluorescence spectroscopy, *Colloids Surf. A*, 2000, 169, 337-350.
- [30] Larsson C., Rodahl M., Hook F., Characterization of DNA immobilization and subsequent hybridization on a 2D arrangement of streptavidin on a biotin-modified lipid bilayer supported on SiO₂, *Anal. Chem.* 2003, 75, 5080-5087
- [31] Schult K., Katerkamp A., Trau D., Grawe F., Cammann K., Meusel M., Disposable optical sensor chip for medical diagnostics: New ways in bioanalysis, *Anal. Chem.*, 1999, 71, 5430-5435
- [32] Schneider B. H., Dickinson E. L., Vach M. D., Hoijer J. V., Howard L. V., Highly sensitive optical chip immunoassays in human serum, *Biosens. Bioelectron.*, 2000, 15, 13–22.
- [33] Boozer C., Yu Q., Chen S., Lee C., Homola J., Yee S. S., Jiang S., Surface functionalization for self-referencing surface plasmon resonance (SPR) biosensors by multi-step self-assembly, *Sens. Actuators B*, 2003, 90, 22–30
- [34] Vareiro M. M. L. M., Liu J., Knoll W., Zak K., Williams D., Toby A., Jenkins A., Surface plasmon fluorescence measurements of human chorionic gonadotrophin: Role of antibody orientation in obtaining enhanced sensitivity and limit of detection, *Anal. Chem.* 2005, 77, 2426-2431
- [35] Xu H., Zhao X., Grant C., Lu J. R., Williams D. E., Penfold J., Orientation of a monoclonal antibody adsorbed at the solid/solution interface: A combined study using atomic force microscopy and neutron reflectivity, *Langmuir*, 2006, 22, 6313-6320
- [36] E.D. Palik (Ed.), *Handbook of Optical Constants of Solids*, Academic Press, Orlando, 1985, p. 290
- [37] E.D. Palik (Ed.), *Handbook of Optical Constants of Solids II*, Academic Press, San Diego, 1991, p. 1059
- [38] Xu H., Lu J. R., Williams D. E., Effect of surface packing density of interfacially adsorbed monoclonal antibody on the binding of hormonal antigen human chorionic gonadotrophin, *J. Phys. Chem. B*, 2006, 110, 1907-1914
- [39] De Feitjer J. A., Benjamins J., Veer F. A., Ellipsometry as a tool to study the ad-sorption of synthetic and biopolymers at the air– water interface, *Biopolymers*, 1978, 17, 1759-1772